


RESEARCH

Open Access



Anti-proliferative activity of RIMHS-Qi-23 against MCF-7 breast cancer cell line is through inhibition of cell proliferation and senescence but not inhibition of targeted kinases

Randa El-Gamal^{1,2,3,4*} , Sara Elfarrash^{2,5}, Mohammad EL-Nablaway^{1,6}, Asmaa Ahmed Salem⁷, Seyed-Omar Zaraei⁸, Hanan S. Anbar⁹, Ashraf Shoma¹⁰ and Mohammed I. El-Gamal^{4,8,11,12*}

Abstract

Background Breast cancer is the most common malignancy globally, and is considered a major cause of cancer-related death. Tremendous effort is exerted to identify an optimal anticancer drug with limited side effects. The quinoline derivative RIMHS-Qi-23 had a wide-spectrum antiproliferative activity against various types of cancer cells.

Methods In the current study, the effect of RIMHS-Qi-23 was tested on MCF-7 breast cancer cell line to evaluate its anticancer efficacy in comparison to the reference compound doxorubicin.

Results Our data suggest an anti-proliferative effect of RIMHS-Qi-23 on the MCF-7 cell line with superior potency and selectivity compared to doxorubicin. Our mechanistic study suggested that the anti-proliferative effect of RIMHS-Qi-23 against MCF-7 cell line is not through targeted kinase inhibition but through other molecular machinery targeting cell proliferation and senescence such as cyclophilin A, p62, and LC3.

Conclusion RIMHS-Qi-23 is exerting an anti-proliferative effect that is more potent and selective than doxorubicin.

Keywords Breast cancer, MCF-7, Quinoline, Anticancer drugs, Raf kinases

*Correspondence:

Randa El-Gamal

drandaelgamal@mans.edu.eg; drandaelgamal@yahoo.com

Mohammed I. El-Gamal

drmelgamal2002@gmail.com; malgamal@sharjah.ac.ae; drmelgamal@mans.edu.eg

¹ Department of Medical Biochemistry & Molecular Biology, Faculty of Medicine, Mansoura University, Mansoura 35516, Egypt

² Medical Experimental Research Center (MERC), Faculty of Medicine, Mansoura University, Mansoura 35516, Egypt

³ Department of Medical Biochemistry, Faculty of Medicine, Horus University, New Damietta, Egypt

⁴ Department of Medical Biochemistry, Faculty of Medicine, University of Mansoura, Mansoura, Al-Daqahlia Governorate 35516, Arab Republic of Egypt

⁵ Department of Medical Physiology, Faculty of Medicine, Mansoura University, Mansoura 35516, Egypt

⁶ Department of Basic Medical Sciences, College of Medicine, AlMaarefa University, PO Box 71666, Riyadh 11597, Kingdom of Saudi Arabia

⁷ Department of Clinical Oncology and Nuclear Medicine, Faculty of Medicine, Mansoura University, Mansoura, Egypt

⁸ Research Institute of Medical and Health Sciences, University of Sharjah, Sharjah 27272, United Arab Emirates

⁹ Department of Clinical Pharmacy and Pharmacotherapeutics, Dubai Pharmacy College for Girls, Dubai 19099, United Arab Emirates

¹⁰ Department of General Surgery, Mansoura Faculty of Medicine, Mansoura University Hospital, Mansoura 35516, Egypt

¹¹ Department of Medicinal Chemistry, College of Pharmacy, University of Sharjah, Sharjah 27272, United Arab Emirates

¹² Department of Medicinal Chemistry, Faculty of Pharmacy, Mansoura University, Mansoura 35516, Egypt



© The Author(s) 2023. **Open Access** This article is licensed under a Creative Commons Attribution 4.0 International License, which permits use, sharing, adaptation, distribution and reproduction in any medium or format, as long as you give appropriate credit to the original author(s) and the source, provide a link to the Creative Commons licence, and indicate if changes were made. The images or other third party material in this article are included in the article's Creative Commons licence, unless indicated otherwise in a credit line to the material. If material is not included in the article's Creative Commons licence and your intended use is not permitted by statutory regulation or exceeds the permitted use, you will need to obtain permission directly from the copyright holder. To view a copy of this licence, visit <http://creativecommons.org/licenses/by/4.0/>. The Creative Commons Public Domain Dedication waiver (<http://creativecommons.org/publicdomain/zero/1.0/>) applies to the data made available in this article, unless otherwise stated in a credit line to the data.

Introduction

Breast cancer (BC) is the most common malignancy in women worldwide [1]. With 0.5 million fatalities and more than two million new cases in 2020, BC is the second most prominent cause of death in women worldwide [2]. The number of BC new cases is expected to increase to more than three million by 2040, according to the International Agency for Research on Cancer (GLOBOCAN) [3]. According to recent reports, developing countries will suffer from two-thirds of the new breast cancer cases by 2035 [4].

The exact cause of cancer development remains unresolved, but it is hinted that various genetic predispositions, alterations in molecular events including uncontrolled cell proliferation [5], cellular transformations, improper regulation of the cell cycle [6], and angiogenesis, along with increased invasion ensuing metastases [7], are all possible factors. The various cellular and enzymatic pathways responsible for growth and proliferation of cancer cells that have been identified acted as an accelerator for the development of novel anticancer drugs, which increased the available treatment options for patients and consequently, upgraded treatment outcomes [4]. Despite the discovery and the clinical use of many effective anticancer agents, most of them, if not all, suffer from serious drawbacks such as severe side effects. Side effects such as nausea, weight loss, fatigue, loss of appetite, and hair loss stem from non-specific target effects, where anticancer drugs are targeting the normal cells in addition to cancer cells, and affecting pathways unrelated to the progression of cancer [8]. Consequently, the anticancer drug development focuses on hunting safer and more effective drug candidates that exert high selectivity toward cancer cells over normal cells to decrease the severity of side effects and toxicity.

We have previously reported a quinoline-based series possessing an anti-proliferative phenotype as c-Raf kinase inhibitors [9–11]. Among the series, several compounds exhibited broad-spectrum anti-proliferative activity on the NCI-60 cancer cell lines and were more selective toward cancer cells in comparison to the WI-38 normal cell line. Additional *in vitro* testing, such as investigating possible mechanisms of action (kinase panel as well as caspase-3/7 and lactate dehydrogenase release assays) and pharmacokinetic properties (aqueous solubility, partition coefficient, and Caco-2 A-B permeability), indicated promising results [11]. In the current study, we have opted to test the compound RIMHS-Qi-23 as a potential anti-breast cancer drug using the MCF-7 cell line. This was selected based on its promising *in vitro* anti-proliferative activity. We also investigated the potential kinase inhibitory effect, molecular mechanisms including cell proliferation, autophagy, and apoptosis as

possible mechanisms of action. RIMHS-Qi-23 structure, synthetic procedures, and spectral analysis charts are provided in the [Supplementary file](#).

Materials and methods

NCI-60 screening

Single-dose testing

A preliminary *in vitro* anticancer assay for the target compound was performed against 60 human tumor cell line panel taken from nine different tissues (Fig. 1) in accordance with the protocol of the Drug Evaluation Branch, NCI, Bethesda, MD. To determine the growth inhibition percentages, the target substance was given to the 60 cell lines under study in the single-dose assay at a concentration of 10 μ M.

Five-dose testing

To assess the potency of RIMHS-Qi-23 and calculate its GI_{50} and TGI values across the 60 cancer cell lines, the compound was tested in a five-dose testing mode. The detailed GI_{50} and TGI values of the compound over each of the tested cell lines for the corresponding cancer type are summarized in Table 1 and Fig. 1.

Anti-proliferative activity

Cell culture

The breast cancer cell line (MCF-7) and normal diploid human fibroblasts (WI-38) were obtained from Medical Experimental Research Center, Faculty of Medicine, Mansoura University and maintained in Dulbecco's Modified Eagle Medium (DMEM, Sigma-Aldrich), 10% (v/v) Fetal Bovine Serum (FBS, Gibco, Thermo-Fisher, 10270106) and 1% (v/v) Penicillin/Streptomycin (Gibco, Thermo-Fisher, 15140122) are added as supplements. Cells were maintained in incubators at 37 °C with 5% CO_2 and 95% relative humidity till reaching 80% confluency.

MTT assay

To determine the chemotherapeutic impact of RIMHS-Qi-23 on the viability of the MCF-7 cancer cells, 3-(4,5-dimethylthiazol-2-yl)-2,5-diphenyltetrazolium bromide assay (MTT) was performed as described earlier in [12]. Briefly, the cell lines were grown in tissue culture plates at a density of 4×10^4 cells per well for an incubation time of 48 h at 37 °C. The incubated plates were treated either with RIMHS-Qi-23, doxorubicin, or as a negative control with dimethylsulfoxide (DMSO) for 48 h. Then, the culture media was discarded and MTT tetrazolium dye (0.5 mg/mL) was added and incubated at 37 °C for 2 h. The formazan crystals formed were dissolved in DMSO, and the absorbance at 570 nm was measured for each group. For advanced tests, the concentration (IC_{50}) needed to reduce viability by 50%

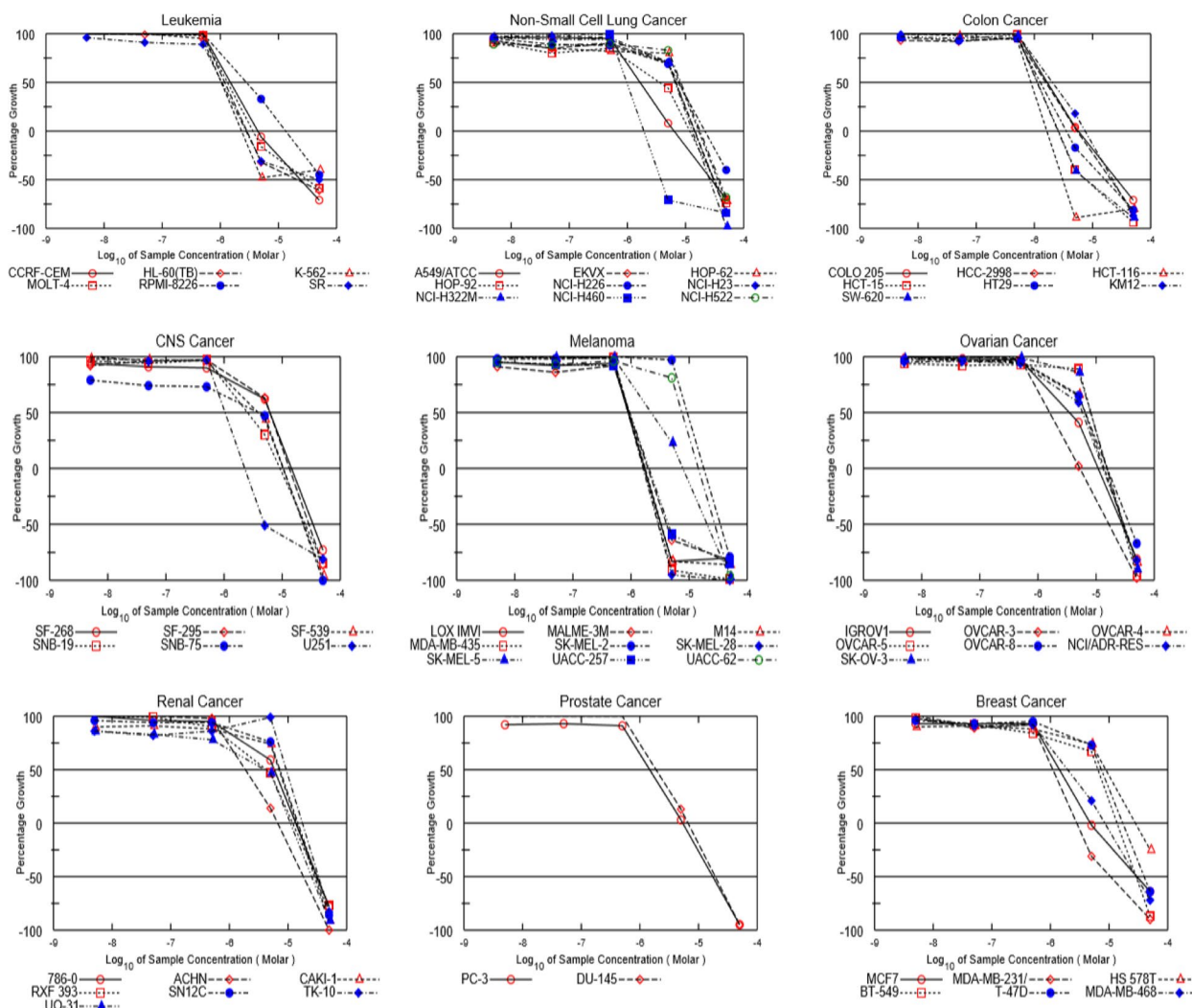


Fig. 1 Dose-response curve of RIMHS-Qi-23 against the NCI 60 cell line panel of nine cancer types; from left to right: Leukemia, Non-small cell lung cancer, Colon cancer, CNS cancer, Melanoma, Ovarian cancer, Renal cancer, Prostate cancer and Breast cancer. For breast cancer cell lines panel, the figure shows the effect on MCF-7, MDA-MB-231, H8 578T, BT-549, T-47D and MDA-MB-468

was identified using the Formula: Percentage of viable cells = A_{570} of treated cells / A_{570} of control cells \times 100. This expression measures the impact of different drug concentrations on the proliferation of cells.

Kinase profiling

RIMHS-Qi-23 was screened using the Kinase HotSpotSM service from Reaction Biology Corp. (<http://www.reactionbiology.com>). The utilized assay procedure is as reported on Reaction Biology Corp. website (<https://www.reactionbiology.com/assay-protocol-hotspot>) using 1 μ M concentration of ATP.

Real time quantitative PCR

After checking the results of MTT assay and calculation of IC_{50} values, the experiment was repeated in triplicates of five serial doses concentration of the tested compound as follows: 20 μ M, 10 μ M, 6.6 μ M, 3.3 μ M, 1.1 μ M versus a triplicate of untreated cells. After 48 h incubation, triplicates of one million cells were collected, immediately homogenized with QIAzol reagent, then RNA and protein extraction (for real-time PCR and western blot, respectively) were immediately started.

Using the QIAzol reagent (Qiagen, Germany), the total cellular RNA was extracted in accordance with the guidelines given by the manufacturer. Thermo

Table 1 GI₅₀ and TGI values (μM) of RIMHS-QI-23 over the NCI-60 cancer cell line panel

Cancer type	Cell line	Tested compound		
		GI ₅₀ ^a	TGI ^b	
Leukemia	CCRF-CEM	1.48	4.39	
	HL-60(TB)	1.18	2.84	
	K-562	1.04	2.31	
	MOLT-4	1.32	3.65	
	RPMI-8226	2.81	13.40	
	SR	1.06	2.75	
Non-small cell lung cancer	A549/ATCC	1.64	6.31	
	EKVX	6.70	14.20	
	HOP-62	7.86	16.80	
	HOP-92	3.58	11.80	
	NCI-H226	7.45	21.40	
	NCI-H23	6.88	14.50	
	NCI-H322 M	6.55	13.00	
	NCI-H460	0.975	1.92	
	NCI-H522	8.25	17.70	
Colon cancer	COLO 205	1.72	5.58	
	HCC-2998	1.56	5.42	
	HCT-116	0.871	1.63	
	HCT-15	1.13	2.59	
	HT29	1.26	3.52	
	KM12	2.04	7.47	
	SW-620	1.11	2.54	
	CNS cancer	SF-268	6.13	14.30
		SF-295	6.10	13.20
SF-539		3.81	10.30	
SNB-19		2.48	9.08	
SNB-75		3.76	10.40	
Melanoma	U251	1.03	2.26	
	LOX IMVI	0.883	1.70	
	MALME-3 M	0.931	7.94	
	M14	0.933	1.76	
	MDA-MB-435	0.907	1.66	
	SK-MEL-2	9.21	17.70	
	SK-MEL-28	0.889	1.61	
	SK-MEL-5	2.19	7.75	
	UACC-257	0.951	2.04	
Ovarian cancer	UACC-62	7.48	14.30	
	IGROV1	3.49	10.90	
	OVCAR-3	1.59	5.25	
	OVCAR-4	6.37	13.70	
	OVCAR-5	8.13	15.10	
	OVCAR-8	6.47	15.40	
	NCI/ADR-RES	5.82	13.20	
SK-OV-3	7.98	15.40		

Table 1 (continued)

Cancer type	Cell line	Tested compound	
		GI ₅₀ ^a	TGI ^b
Renal Cancer	786-0	5.84	13.50
	ACHN	1.85	6.61
	CAKI-1	6.95	14.00
	RXF 393	4.27	11.90
	SN12C	7.21	14.70
	TK-10	9.29	17.50
Prostate Cancer	UO-31	4.07	11.00
	PC-3	1.46	5.37
Breast Cancer	DU-145	2.00	6.63
	MCF-7	1.43	4.82
	MDA-MB-231/ATCC	1.09	2.78
	HS 578T	8.77	28.00
	BT-549	6.47	13.70
	T-47D	7.36	17.00
	MDA-MB-468	1.96	8.48

^a GI₅₀ is the concentration that produces 50% inhibition of the cell growth

^b TGI is the concentration that produces 100% inhibition

Scientific’s NanoDrop One (USA) was used to measure the amount of RNA present. One μg of RNA was reverse transcribed using the Bioline cDNA synthesis kit (Bioline, USA). A total of 20 μL was used in quantitative real-time PCR (qRT-PCR) [10 μl of HERA SYBR green PCR Master Mix (Willowfort, UK), 1 μl of cDNA template, 2 μl (10 pmol/ μl) of each gene primer and 7 μl of nuclease-free water] utilizing a real-time PCR thermocycler (Azure Cielo 6, Azure, USA). The thermal profile was set at 95 °C for 2 min, followed by 40 cycles of denaturation at 95 °C for 10 s, then annealing and extension at 60 °C for 30 s. Table 2 lists the primer pair sequences that were employed. Glyceraldehyde-3-phosphate dehydrogenase (GAPDH) was used as a control gene. The primer sets were allocated using the Primer 3 software (version 4.1.0), and the Primer-BLAST program (<https://www.ncbi.nlm.nih.gov/tools/primer-blast/>) was used to evaluate the specificity of the primer sets. An examination of the melting curve of the PCR products was done to determine their specificity. From Vivantis (Vivantis Technologies, Malaysia), primer sets were purchased. The subsequent equation was used to assess the fold change of gene expression using the 2^{-ΔΔCT} method, with ΔCt = Ct target gene - Ct control gene [13].

Table 2 The sequence of primers used in qRT-PCR analysis

Gene	Sequence	Product size	RefSeq
BCL2 associated X, apoptosis regulator (BAX)	Forward: AGCTGCAGAGGATGATTGCC Reverse: CCCCAGTTGAAGTTGCCGTC	100 bp	NM_001291428.1
B-cell lymphoma 2 (BCL2)	Forward: TGTGTGTGGAGAGCGTCAAC Reverse: CTACCCAGCCTCCGTTATCC	120 bp	NM_000657.2
Protein 53 (P53)	Forward: GAGCTGAATGAGGCCTTGGA Reverse: CTGAGTCAGGCCCTTCTGTCTT	151 bp	NM_000546.6
Protein 21 (p21)	Forward primer: GACCAGCATGACAGATTTC Reverse primer: TGAGACTAAGGCAGAAGATG	141 bp	NM_000389.5
Marker Of Proliferation Ki-67 (Ki-67)	Forward primer: AATCCAACCTCAAGTAAACGGGG Reverse primer: TTGGCTTGCTTCCATCCTCA	127 bp	NM_002417.5
Glyceraldehyde-3-phosphate dehydrogenase (GAPDH)	Forward primer: CTCTGCTCCTCCTGTTTCGAC Reverse primer: GCGCCCAATACGACCAAATC	121 bp	NM_002046.7

Immunoblotting

The total protein extraction from cells was performed by QIAzol reagent (Qiagen, Germany) immediately after obtaining the cells. Protein concentration was measured by Bradford assay (Bosterbio, Canada). Equal amounts of proteins (20 µg) were then separated on SDS-PAGE and transferred to 0.22 mm nitrocellulose membrane (Abcam, USA) using Eco-Line Biometra apparatus (Gottingen, Germany). Page Ruler pre-stained protein ladder 10–180 kDa (ThermoFisher, USA) was used as the molecular size marker. Membranes were then handled as described earlier in [14]. Briefly, the membrane was incubated in 5% non-fat milk for 1 h at room temperature as a blocking agent with gentle shaking. Primary antibodies against LC3B (GeneTex catalog no. GTX127375, dilution 1:1000), p62 (SantaCruz Biotechnology catalog no. sc-48389, dilution 1:500), cyclophilin A (Cell signaling catalog no. 2175, dilution 1:1000) and β-actin (Abcam ab227387, dilution 1:5000) were incubated overnight at 4 °C. After three times of 15 min washing each with TBS-Tween, the membranes were incubated with peroxidase-coupled goat anti-rabbit IgG (Santa Cruz Biotechnology, USA) at 37 °C for 2 h. Membranes were then visualized (after 3 × 15 min washing with TBS-Tween) using chemiluminescent substrate (Clarity™ WesternECL substrate, Catalog no. 1705061, Bio-Rad, USA) and the chemiluminescent signals were collected using Chemi-Doc MP imager. Image analysis software was used to

quantify the band intensity after normalization to β-actin bands signals.

Statistical analysis

Using the 2017 release of IBM Corp.'s SPSS program, data were entered and examined. Armonk, New York: IBM Corp., IBM SPSS Statistics for Windows, Version 25.0. Shapiro-Wilk's test was used to initially check the normality of quantitative data; if $p > 0.05$, the data were considered to be normally distributed; otherwise, they were not. By looking at boxplots, the existence of significant outliers was tested. When quantitative data were normally distributed, they were reported as mean ± standard error (SE). Six study cell groups' quantitative data were compared using the One-Way ANOVA test, and then each pair of data were appropriately compared using the post-hoc test. Results are expressed as letters (similar letters = insignificant difference, different letters = significant difference). Tukey adjustment was used as assumption of equal variances were assumed. p value < 0.05 was considered statistically significant.

Results

RIMHS-Qi-23 shows promising results using NCI-60 cell lines and in comparison, to reference drug doxorubicin

Screening RIMHS-Qi-23 on 60 cancer cell lines showed promising results on single-dose testing mode. It was selected for five-dose testing mode to determine its GI_{50}

and TGI values over the 60 cancer cell lines and was reported in comparison to doxorubicin. RIMHS-Qi-23 produced high potency against most of the cell lines (Fig. 1 and Table 1).

RIMHS-Qi-23 shows higher potency and selectivity using MCF-7 and WI-38 cancer cell lines

To evaluate the cytotoxicity of RIMHS-Qi-23, we compared its effect on the widely used MCF-7 breast cancer cell line versus WI-38 normal cells to explore safety and selectivity. RIMHS-Qi-23 was first tested in triplicates of single dose concentration of 10 μM, using doxorubicin as a reference compound, and based on the results of MTT assay, the compound showed higher potency and selectivity. To calculate IC₅₀, both drugs were further tested in five serial doses concentrations as follow: 10, 3.3, 1.1, 0.37, and 0.12 μM on both cell lines. However, the concentration of 10 μM failed to reach 50% inhibition in WI-38. Therefore, we opted for three higher concentrations; 20, 30, and 40 μM to draw the dose-response curve and calculate the IC₅₀ (Fig. 2).

RIMHS-Qi-23 did not exhibit inhibitory activity on a panel of 50 kinases

RIMHS-Qi-23 was tested in a single dose at concentration of 1 μM against a panel of 50 kinases to investigate a possible molecular mechanism through kinase inhibition and evaluate off-target activity. Results shown in Table 3, surprisingly show that RIMHS-Qi-23 did not

exhibit any sufficient inhibitory activity (more than 50%) against any of the tested kinases. On the contrary, previously reported quinoline derivatives from this series were reported as potent c-Raf inhibitors.

RIMHS-Qi-23 influences cell proliferation and senescence but not cell apoptosis

RIMHS-Qi-23's cytotoxic activity against MCF-7 cell line prompted us to investigate possible mechanism of action through screening the inhibition of genes expression responsible for cell apoptosis; (BAX and BCL2), cell senescence; (p53 and p21) and cell proliferation; Ki67 by real-time PCR. There was a statistically significant difference between the studied concentrations and their effect on p53, p21 and ki-67 genes expression (*p* < 0.001, 0.018 and 0.001, respectively), but RIMHS-Qi-23 treatment did not affect the expression of neither BAX pro-apoptotic gene, nor BCL2 anti-apoptotic genes (*p* = 0.131 and 0.145, respectively), as shown in Fig. 3.

RIMHS-Qi-23 exhibits its effect through enhancing the autophagy and necrosis pathways

RIMHS-Qi-23's effect on autophagy pathway and necroptosis pathway was investigated. LC3 and p62 proteins expression were measured to study the effect on autophagy pathway, and cyclophilin A protein expression for necroptosis pathway using western blotting. There was a statistically significant difference between the studied concentrations and their effect on LC3, p62

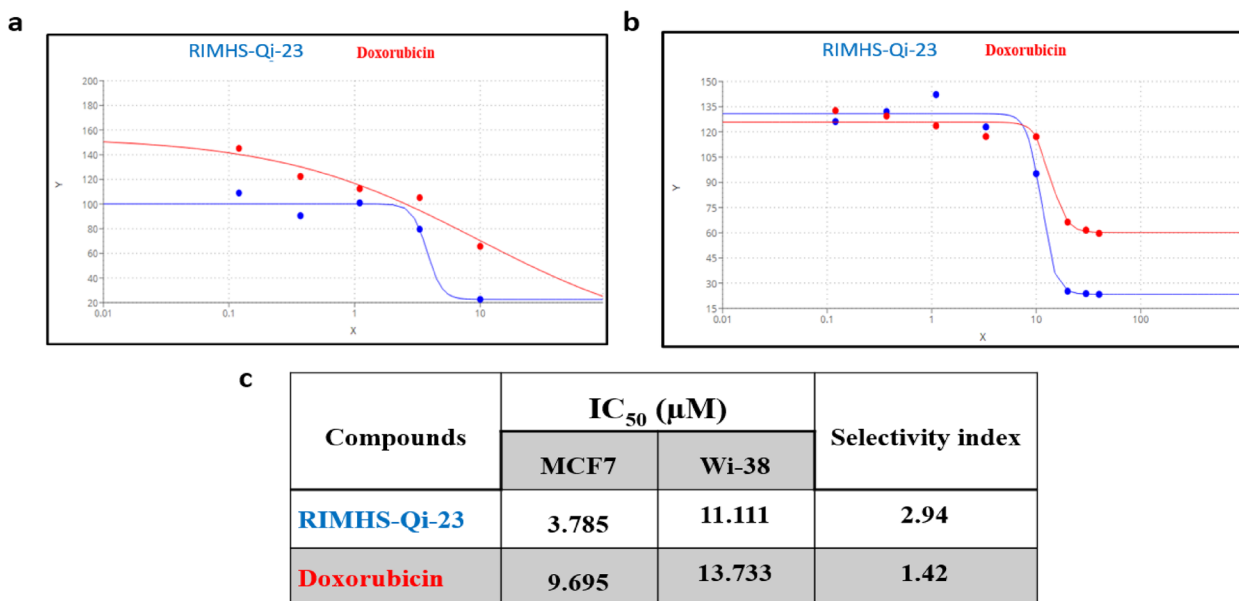


Fig. 2 Cytotoxicity assessment of RIMHS-Qi-23 and reference drug doxorubicin using MCF-7 and Wi-38. **a** Dose response curve showing the cell viability using MCF-7 cell line. **b** Dose response curve for both drugs using Wi-38 cell lines. **c** IC₅₀ values of both compounds in MCF-7 and WI-38 cell lines

Table 3 Residual activity (%) of the panel of 50 kinases after treatment with the RIMHS-Qi-23

Tested kinase	RIMHS-Qi-23 Conc. 1 μM ^a	Tested kinase	RIMHS-Qi-23 Conc. 1 μM ^a
Abl(h)	105	Flt4(h)	101
Abl(T315I)(h)	107	Fms(h)	100
A-Raf(h)	96	GSK3α(h)	110
Aurora-A(h)	107	GSK3β(h)	123
Aurora-B(h)	64	JAK1(h)	110
Aurora-C(h)	113	JAK2(h)	127
B-Raf(h)	91	JAK3(h)	107
B-Raf(V599E)(h)	103	JNK1α1(h)	103
cKit(h)	87	JNK2α2(h)	105
c-Raf(h)	79	JNK3(h)	94
cSRC(h)	108	KDR(h)	102
EGFR(h)	137	MEK1(h)	102
EGFR(L858R)(h)	98	MEK2(h)	113
EGFR(L861Q)(h)	93	MEKK2(h)	104
EGFR(T790M)(h)	129	MEKK3(h)	110
EGFR(T790M,L858R)(h)	104	Met(h)	97
ErbB2(h)	104	mTOR(h)	97
ErbB4(h)	96	PDGFRα(h)	93
FGFR1(h)	110	PDGFRβ(h)	114
FGFR2(h)	105	Pim-1(h)	94
FGFR3(h)	103	Ros(h)	125
FGFR4(h)	93	TrkA(h)	114
Flt1(h)	121	TrkB(h)	117
Flt3(D835Y)(h)	87	TrkC(h)	97
Flt3(h)	80	PI3 Kinase (p120g)(h)	96

^a Residual activity of the kinase after treatment with 1 μm of the compound; inhibition percentage = 100-residual activity

and cyclophilin A proteins expression ($p < 0.001$ for all). RIMHS-Qi-23 inhibited MCF-7 viability via upregulation of LC3, downregulation of p62, and/or upregulation of the necroptotic cyclophilin A protein expression. All proteins, LC3, p62, and cyclophilin A expressions were highly demonstrated at concentration of 20 μM, but lower at concentration of 10 μM, 6.6 μM, 3.3 μM and 1.1 μM, respectively as shown in Fig. 4.

Discussion

Breast cancer is the most common malignancy in women, and it is responsible for the highest number of cancer-related deaths in women worldwide [15]. Present therapeutic strategies against breast cancer have different reported side effects including allergies, weight and hair loss, recurrence of cancer, and emergence of drug resistance [16]. Doxorubicin is part of the anthracycline family and is currently considered as the most effective

chemotherapeutic drug for breast cancer treatment [17]. However, side effects, drug resistance, and tumor growth result in poor patient prognosis and survival [18]. Collectively, the need to identify a safer, more effective, and more specific alternative is increasing.

In the present study, the compound RIMHS-Qi-23 was selected for cytotoxic studies as an anti-proliferative agent. The data from dose response curve, where RIMHS-Qi-23 was tested on different NCI-60 cell line panel of nine cancer types suggested that it exhibits a promising potent effect against most of cell lines.

Because of the promising results of RIMHS-Qi-23 compound on MCF-7 cancer cell type, and in addition to authors' interest in this type of cancer (non-invasive & hormone-dependent), a more in-depth study of the effect and mechanism of action of RIMHS-Qi-23 compound was done.

Initial cytotoxicity screening of this compound on the breast cancer cell line MCF-7 displayed significant anti-cancer activities in a dose- and time- dependent manner. RIMHS-Qi-23 showed a lower IC₅₀ than doxorubicin, indicating a greater potency and selectivity (i.e., a higher selectivity index, for MCF-7 cancer cells in comparison to doxorubicin).

To explore the potential mechanism by which RIMHS-Qi-23 is exhibiting its anticancer effect on breast cancer cell line, the compound was tested on a panel of 50 kinases to assess its influence on the activities of different kinases. Although previous quinoline derivatives from the same series exhibited c-Raf inhibitory activity, data did not demonstrate any promising kinase inhibitory effect over the 50 tested kinases. The compound effect was more evident on Aurora-B and c-Raf among others. However, it failed to reach at least a 50% reduction at μM concentration against them. A powerful and broad-spectrum anti-proliferative effect was seen on NCI-60 cell lines by the strongest c-Raf inhibitor in the prior series, which had an IC₅₀ of 0.067 μM. The anti-proliferative activity of RIMHS-Qi-23 is comparable and, in some instances, even exhibited superior GI₅₀, as shown in Table 2 (NSCLC A549 & NCI-H460, Colon HCC-2998, HCT-116, HT29, & SW-620, CNS U251, Melanoma LOX IMVI, MALME-3 M, M14, MDA-MB-435, SK-MEL-28, & UACC-257, and breast MDA-MB-231) in comparison to the previous series. We believe that RIMHS-Qi-23's anti-proliferative and kinase activity suggests an off-target effect which is possibly shared with previous quinoline compounds based on high structural similarity it possesses compared with the previous series.

To further investigate the molecular mechanism behind the cytotoxic effect of the drug, the influence of the drug on genes expression levels involved in cancer related signaling pathways, such as apoptosis, cell

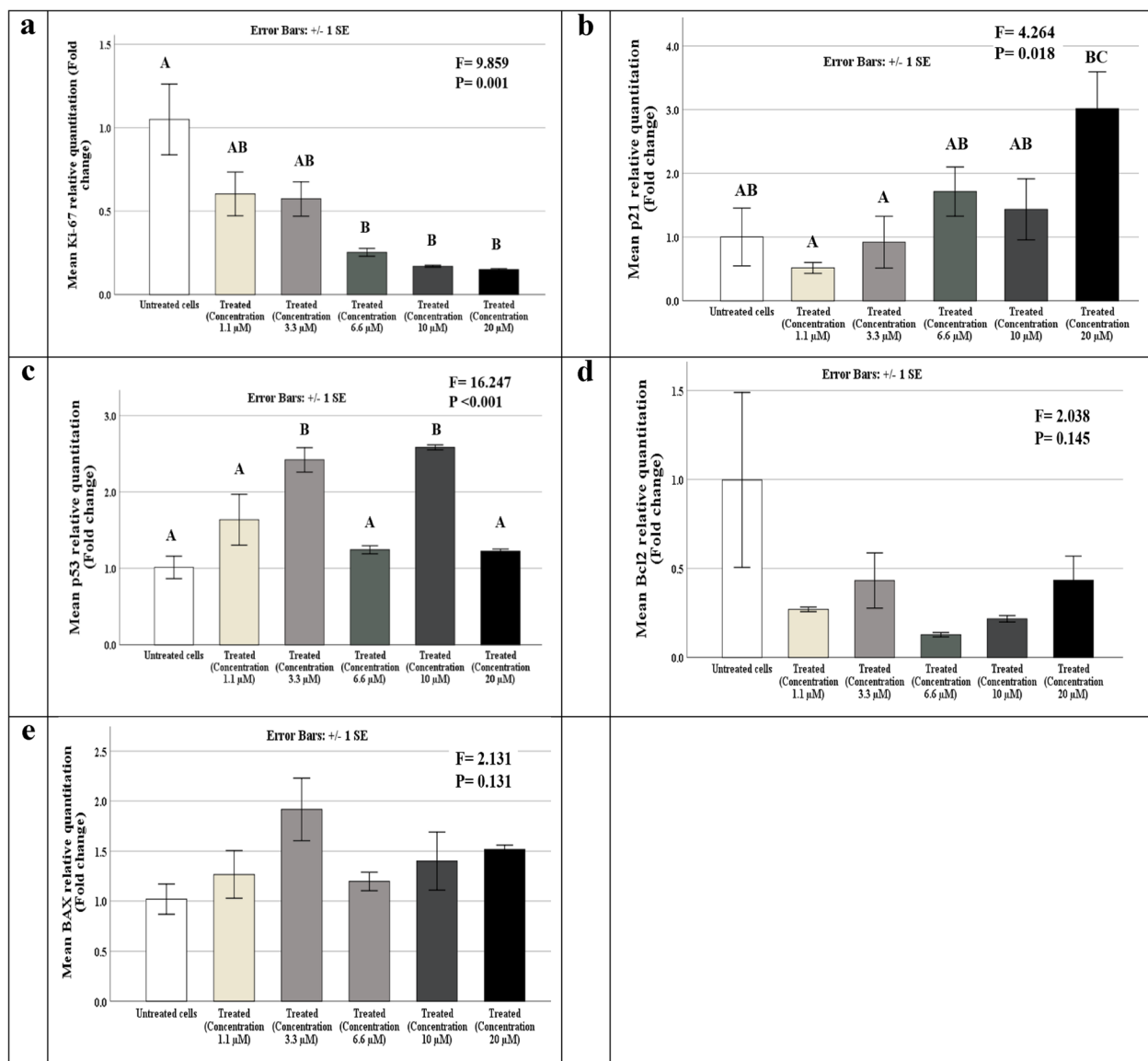


Fig. 3 RIMHS-Qi-23 acts through affecting mRNA expression regulation of cell senescence and proliferation genes but not pro or anti apoptosis genes as studied by real-time PCR. **a** Effect of different concentrations (1.1, 3.3, 6.6, 10, 20 μM) on relative expression of Ki-67 mRNA level, showing significant reduction of mRNA expression level **b** p21 **c** p53 **d** Bcl-2 **e** BAX. Data are represented as mean ± standard error of gene expression fold changes of cells' triplicates, Capital letters are used to denote *p* values from One-Way ANOVA followed by a post-hoc test (similar letters = a statistically non-significant difference, while different letters = a statistically significant difference). *P* values utilizing Tukey adjustment are bolded to denote significant *p* values (≤ 0.05)

senescence and cell proliferation were evaluated by qRT-PCR. Five different concentrations ranging from 1.1 to 20 μM were investigated in the current setup. A dose-dependent reduction of cell proliferative Ki-67 mRNA expression suggests that RIMHS-Qi-23 can hinder the proliferation of cancer cells in comparison to healthy cells. Ki-63 is considered as one of the most controversial markers when discussing the treatment decision on breast cancer. Since Ki-67 can be

seen during all the cell cycle active phases but is not found in dormant cells, it has become a superb option for measuring the growth fraction of a particular cell population. The ability of RIMHS-Qi-23 to hinder its expression can suggest it as a potential candidate to improve cancer prognosis through inhibition of cancer cell proliferation. To the best of our knowledge, there is no study that has reported the effect of doxorubicin on expression of Ki-67 up to the time of writing this study.

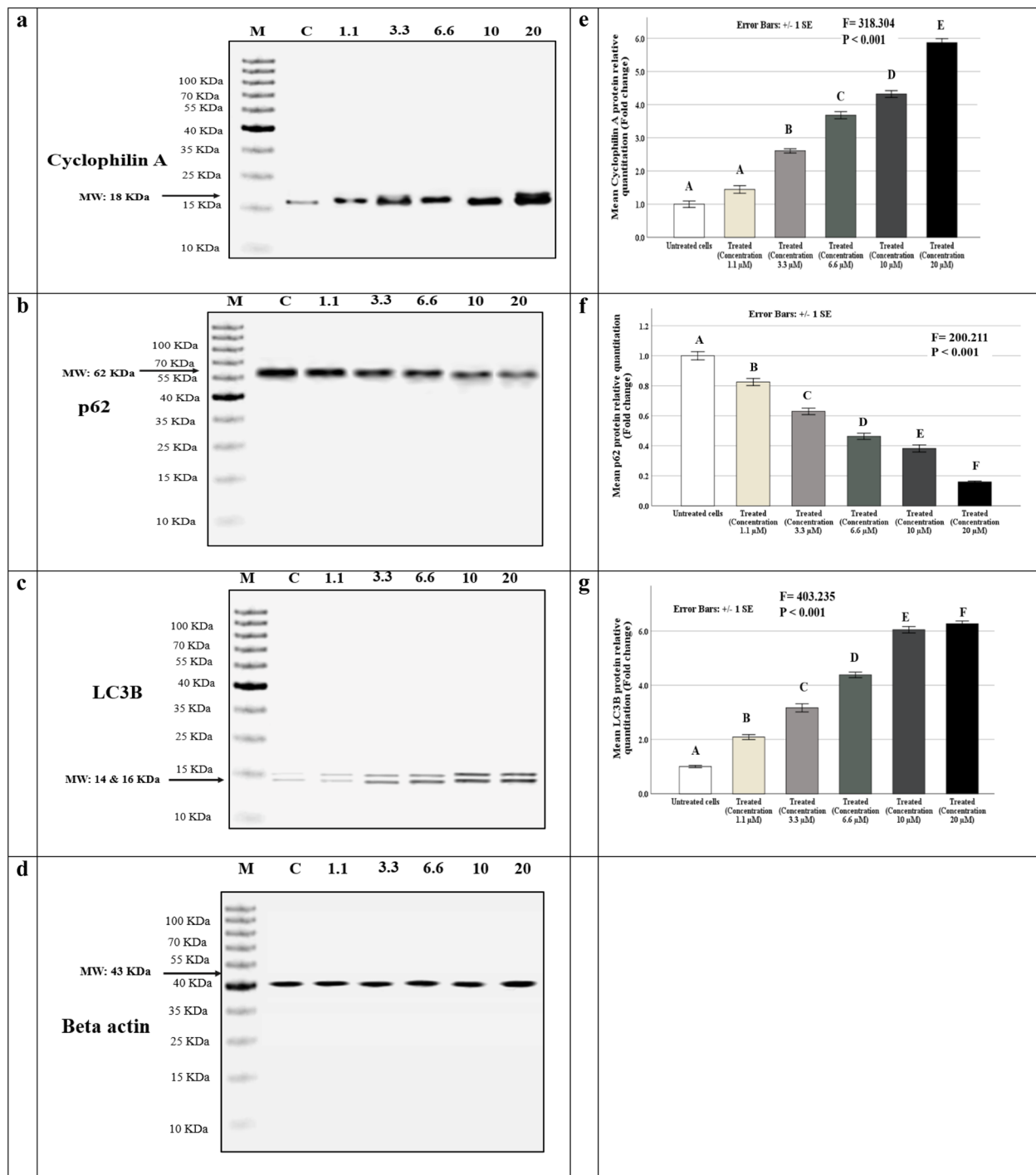


Fig. 4 RIMHS-Qi-23 acts through affecting autophagy and necrosis pathways: **a-d** Immunoblotting of MCF-7 cell lines homogenates following treatment with serial concentration, incubated with cyclophilin A, p62, LC3 and β -actin as loading control **e-g** Quantification of immunoblots band values relative to β -actin were normalized to non-treated cells and represent mean \pm SEM. Capital letters represent *p* values from One-Way ANOVA followed by a post-hoc test (similar letters = a statistically non-significant difference, while different letters = a statistically significant difference). Bold values denote significant *p* values (≤ 0.05)

Assessment of the p53/p21 signaling pathway that plays a central role of cellular senescence [19], revealed that RIMHS-Qi-23 treatment showed upregulation of both genes' mRNA expression levels. Cellular senescence has been considered as a powerful tumor suppressive mechanism [20]. Senescent cells can potentially cause tissue malfunction and/or poor outcomes by secreting pro-inflammatory cytokines that have a detrimental effect on the tissue microenvironment and the nearby cells [21]. Induction of the cellular senescence via p53-dependent pathway is one of the mechanisms which explore the anti-tumor effect of doxorubicin [22]. The effect of treatment on p53/p21 signaling was more evident at higher drug concentrations for p21 in a dose-dependent manner. The effect of the drug on p53 was not very well understood and needs further justification. An initial upregulation was evident at a drug concentration of 3.3 and 10 μ M but failed to reach statistical significance in the treated groups at concentration of 6.6 and 20 μ M. Upregulation of p53 was reported to be associated with better prognosis via increasing tumor cells sensitivity to the growth inhibitory effect of progesterone [23] suggesting another possible mechanism by which our compound exhibits an anticancer effect on MCF-7 cell line.

Lastly, to evaluate the effect of the compound on the apoptosis pathway, BAX and BCL2 gene expression levels were examined. Our data showed that treatment did not have any influence on their expression levels, which means that the effect of the compound is unlikely to be achieved through regulation of the pro-apoptotic or anti-apoptotic proteins. Our finding contrasts with an earlier report that showed that doxorubicin exhibits its anticancer effect through the reduction of anti-apoptotic genes and elevation of pro-apoptotic genes [24].

Under various stressful circumstances, autophagy is a crucial process in cell recycling and the breakdown of resources for cell homeostasis [25]. Protein light chain 3 (LC3) and p62/SQSTM1 (p62) are associated with autophagosomal membranes that engulf cytoplasmic content for subsequent degradation [26]. Both LC3 and p62 are frequently used as markers to assess autophagy [27]. Treated MCF-7 cells with RIMHS-Qi-23 revealed an increase in LC3 protein expression and reduction of p62, which indicate activated autophagy in cancer cells and inhibited cell proliferation. This substantiates other findings that indicate that autophagy is induced in MCF-7 cells with many anticancer compounds like flavopiridol [28], ursolic acid [29], and baicalein [30]. Moreover, an increased expression of cyclophilin A in the current study suggests that the drug induces the necroptosis pathway as an additional anticancer

mechanism. Necroptosis is a controlled form of necrosis in which dead cells burst and release internal substances that may cause an innate immune reaction [31].

Conclusion

In conclusion, our data suggest that RIMHS-Qi-23 is exerting an anticancer effect, which is more potent and selective than doxorubicin, on the non-invasive, hormone-dependent type of breast cancer (MCF-7). Mechanistic studies have revealed that the compound's anticancer effect is via a different mechanism apart from its role as a c-Raf kinase inhibitor. The data suggest the involvement of autophagy and necroptosis pathways via regulation of cyclophilin A, p62, p53/p21, and LC3 among others.

Recommendations

The authors investigated the effect of RIMHS-Qi-23 compound on MCF-7 breast cancer cells being non-invasive type of cancer and hormone-dependent. Further studies will be needed to complement our findings and to further accommodate RIMHS-Qi-23 as a possible anticancer drug candidate, considering its potency and superior selectivity with other standard drugs and performing more extensive research for the possible mechanism(s) of action on several types of cancer cells.

Abbreviations

BAX	BCL2 associated X, apoptosis regulator
BC	Breast cancer
BCL2	B-cell lymphoma 2
cDNA	Complementary DNA
C-RAF	Cellular-rapidly accelerated fibrosarcoma
Ct	Cycle of threshold
DMEM	Dulbecco's Modified Eagle Medium
FBS	Fetal Bovine Serum
GAPDH	Glyceraldehyde-3-phosphate dehydrogenase
GI ₅₀	The concentration that produces 50% inhibition of the cell growth
IC50	The concentration needed to reduce viability by 50%
Ki-67	Marker Of Proliferation
LC3	Protein light chain 3
MCF-7	Acronym of Michigan Cancer Foundation-7, referring to the institute where the cell line was established
MTT	3-(4,5-dimethylthiazol-2-yl)-2,5-diphenyltetrazolium bromide assay
NCI-60	A group of 60 human cancer cell lines used by the National Cancer Institute (NCI)
p21	Protein 21
p53	Protein 53
P62	Protein 62
qRT-PCR	Quantitative real-time PCR
RIHMS-Qi-23	Research Institute for Medical and Health Sciences – Quinoline derivative
RNA	Ribonucleic acid
SE	Standard error
TGI	The concentration that produces 100% inhibition
WI-38	Wistar Institute foetus 38; normal lung fibroblasts

Supplementary Information

The online version contains supplementary material available at <https://doi.org/10.1186/s12885-023-11547-1>.

Additional file 1.

Acknowledgements

The authors are grateful for University of Sharjah, UAE, for financially supporting the chemical synthesis phase of this study (grant No. 2101110153 & 2201110169).

Authors' contributions

"R.E.: Performed cell culture, MTT assay, molecular analysis by real-time PCR & western blotting, statistically analyzed and interpreted data. S.E.: Performed cell culture, MTT assay, analyzed and interpreted data. M.E.: Performed cell culture, MTT assay, molecular analysis by real-time PCR & western blotting. A.A.S.: Analysis and interpretation of data. S.O.Z.: Performed the chemical synthetic phase of the study. H.S.A.: Analysis and interpretation of data. A.S.: Analysis and interpretation of data. M.I.E.: Performed the chemical synthetic phase of the study & kinase profiling. All authors have shared in writing, read and approved the final manuscript."

Funding

The chemical synthesis phase of this study was financially supported by University of Sharjah, UAE (grant No. 2101110153 & 2201110169).

Availability of data and materials

The datasets used and/or analyzed during the current study are available from the corresponding author on reasonable request.

Declarations

Ethics approval and consent to participate

Not applicable as MCF-7 and WI-38 are not primary cell lines, and the authors used commercial, standard cell line (not human tissue samples) that doesn't need ethical approval.

Consent for publication

Not applicable.

Competing interests

The authors declare no competing interests.

Received: 29 July 2023 Accepted: 18 October 2023

Published online: 02 November 2023

References

- Katsura C, Ogunmwoyoni I, Kankam HK, Saha S. Breast cancer: presentation, investigation and management. *Br J Hosp Med (Lond)*. 2022;83(2):1–7. <https://doi.org/10.12968/hmed.2021.0459>.
- International agency for research on cancer, global cancer observatory. 2020. Available from: <http://gco.iarc.fr/>.
- Sung H, Ferlay J, Siegel RL, Laversanne M, Soerjomataram I, Jemal A, Bray F. Global cancer statistics 2020: GLOBOCAN estimates of incidence and mortality worldwide for 36 cancers in 185 countries. *CA Cancer J Clin*. 2021;71(3):209–49. <https://doi.org/10.3322/caac.21660>.
- Ismail H, Shibani M, Zahrawi HW, Slitin AF, Alzabibi MA, Mohsen F, Armashi H, Bakr A, Turkmani K, Sawaf B. Knowledge of Breast cancer among medical students in Syrian Private University, Syria: a cross-sectional study. *BMC Med Educ*. 2021;21(1):251. <https://doi.org/10.1186/s12909-021-02673-0>.
- Nepali K, Sharma S, Sharma M, Bedi PM, Dhar KL. Rational approaches, design strategies, structure activity relationship and mechanistic insights for anticancer hybrids. *Eur J Med Chem*. 2014;77:422–87. <https://doi.org/10.1016/j.ejmech.2014.03.018>.
- Fortin S, Bérubé G. Advances in the development of hybrid anticancer drugs. *Expert Opin Drug Discov*. 2031;8:1029–47. <https://doi.org/10.1517/17460441.2013.798296>.
- Raj T, Bhatia RK, Kapur A, Sharma M, Saxena AK, Ishar MP. Cytotoxic activity of 3-(5-phenyl-3H-[1,2,4]dithiazol-3-yl)chromen-4-ones and 4-oxo-4H-chromene-3-carbothioic acid N-phenylamides. *Eur J Med Chem*. 2010;45(2):790–4. <https://doi.org/10.1016/j.ejmech.2009.11.001>.
- Burdall SE, Hanby AM, Lansdown MR, Speirs V. Breast cancer cell lines: friend or foe? *Breast Cancer Res*. 2003;5(2):89–95. <https://doi.org/10.1186/bcr577>.
- El-Gamal MI, Khan MA, Abdel-Maksoud MS, Gamal El-Din MM, Oh CH. A new series of diarylamides possessing quinoline nucleus: synthesis, in vitro anticancer activities, and kinase inhibitory effect. *Eur J Med Chem*. 2014;87:484–92. <https://doi.org/10.1016/j.ejmech.2014.09.068>.
- El-Gamal MI, Khan MA, Tarazi H, Abdel-Maksoud MS, Gamal El-Din MM, Yoo KH, Oh CH. Design and synthesis of new RAF kinase-inhibiting antiproliferative quinoline derivatives. Part 2: Diarylurea derivatives. *Eur J Med Chem*. 2017;127:413–23. <https://doi.org/10.1016/j.ejmech.2017.01.006>.
- Zaraei SO, Al-Ach NN, Anbar HS, El-Gamal R, Tarazi H, Tokatly RT, Kalla RR, Munther MA, Wahba MM, Alshihabi AM, Shehata MK, Sbenati RM, Shahin AI, El-Awady R, Al-Tel TH, El-Gamal MI. Design and synthesis of new quinoline derivatives as selective C-RAF kinase inhibitors with potent anticancer activity. *Eur J Med Chem*. 2022;238:114434. <https://doi.org/10.1016/j.ejmech.2022.114434>.
- Emam AA, Abo-Elkhaïr SM, Sobh M, El-Sokkary AMA. Role of exopolysaccharides (EPSs) as anti-mir-155 in cancer cells. *Heliyon*. 2021;7(4):e06698. <https://doi.org/10.1016/j.heliyon.2021.e06698>.
- Livak KJ, Schmittgen TD. Analysis of relative gene expression data using real-time quantitative PCR and the 2⁻(Delta Delta C(T)) method. *Methods*. 2001;25(4):402–8. <https://doi.org/10.1006/meth.2001.1262>.
- Elfarrash S, Jensen NM, Ferreira N, Schmidt SI, Gregersen E, Vestergaard MV, Nabavi S, Meyer M, Jensen PH. Polo-like kinase 2 inhibition reduces serine-129 phosphorylation of physiological nuclear alpha-synuclein but not of the aggregated alpha-synuclein. *PLoS One*. 2021;16(10):e0252635. <https://doi.org/10.1371/journal.pone.0252635>.
- Bray F, Ferlay J, Soerjomataram I, Siegel RL, Torre LA, Jemal A. Global cancer statistics 2018: GLOBOCAN estimates of incidence and mortality worldwide for 36 cancers in 185 countries. *CA Cancer J Clin*. 2018;68(6):394–424. <https://doi.org/10.3322/caac.21492>.
- Kushwaha PP, Singh AK, Prajapati KS, Shuaib M, Fayed S, Bringmann G, Kumar S. Induction of apoptosis in Breast cancer cells by naphthylisoquinoline alkaloids. *Toxicol Appl Pharmacol*. 2020;409:115297. <https://doi.org/10.1016/j.taap.2020.115297>.
- Shi Y, Bieerkehazhi S, Ma H. Next-generation proteasome inhibitor oprozomib enhances sensitivity to doxorubicin in triple-negative breast cancer cells. *Int J Clin Exp Pathol*. 2018;11(5):2347–55 PMID: 31938346; PMCID: PMC6958235.
- Shukla A, Hillegass JM, MacPherson MB, Beuschel SL, Vacek PM, Pass HI, et al. Blocking of ERK1 and ERK2 sensitizes human mesothelioma cells to doxorubicin. *Mol Cancer BioMed Central Ltd*. 2010;9(314):1–13. <https://doi.org/10.1186/1476-4598-9-314>.
- Kumari R, Jat P. Mechanisms of cellular senescence: cell cycle arrest and senescence associated secretory phenotype. *Front Cell Dev Biol*. 2021;9:645593. <https://doi.org/10.3389/fcell.2021.645593>.
- Bartkova J, Rezaei N, Liontos M, Karakaidos P, Kletsas D, Issaeva N, et al. Oncogene-induced senescence is part of the tumorigenesis barrier imposed by DNA damage checkpoints. *Nature*. 2014;444(7119):633–7. <https://doi.org/10.1038/nature05268>.
- Mijit M, Caracciolo V, Melillo A, Amicarelli F, Giordano A. Role of p53 in the regulation of cellular senescence. *Biomolecules*. 2020;10(3):420. <https://doi.org/10.3390/biom10030420>.
- El-Far AH, Darwish NHE, Mousa SA. Senescent colon and breast cancer cells induced by doxorubicin exhibit enhanced sensitivity to curcumin, caffeine, and thymoquinone. *Integr Cancer Ther*. 2020;19:1534735419901160. <https://doi.org/10.1177/1534735419901160>.
- Alkhalaf M, El-Mowafy AM. Overexpression of wild-type p53 gene renders MCF-7 breast cancer cells more sensitive to the antiproliferative effect of

- progesterone. *J Endocrinol.* 2003;179(1):55–62. <https://doi.org/10.1677/joe.0.1790055>.
24. Sharifi S, Barar J, Hejazi MS, Samadi N. Doxorubicin changes Bax / Bcl-xL ratio, caspase-8 and 9 in breast cancer cells. *Adv Pharm Bull.* 2015;5(3):351–9. <https://doi.org/10.15171/apb.2015.049>.
 25. Elsayed H, El-Gamal R, Rabei MR, Elhadidy MG, Hamed B, Elshaer M, et al. Enhanced autophagic flux, suppressed apoptosis and reduced macrophage infiltration by dasatinib in kidneys of obese mice. *Cells.* 2022;11(4):746. <https://doi.org/10.3390/cells11040746>.
 26. Schläfli AM, Adams O, Galván JA, Gugger M, Savic S, Bubendorf L, Schläfli AM, Adams O, Galván JA, Gugger M, Savic S, Bubendorf L, Schmid RA, Becker K-F, Tschan MP, Langer R, Berezowska S. Prognostic value of the autophagy markers LC3 and p62/SQSTM1 in early-stage non-small cell Lung cancer. *Oncotarget.* 2016;7(26):39544–55. <https://doi.org/10.18632/oncotarget.9647>.
 27. Klionsky DJ, Abdelmohsen K, Abe A, Abedin MJ, Abeliovich H, Arozena A, et al. Guidelines for the use and interpretation of assays for monitoring autophagy (3rd edition). *Autophagy.* 2016;12:1–222. <https://doi.org/10.1080/15548627.2015.1100356>.
 28. Wang S, Wang K, Wang H, Han J, Sun H. Autophagy is essential for flavopiridol-induced cytotoxicity against MCF-7 breast cancer cells. *Mol Med Rep.* 2017;16(6):9715–20. <https://doi.org/10.3892/mmr.2017.7815>.
 29. Zhao C, Yin S, Dong Y, Guo X, Fan L, Ye M, Hu H. Autophagy-dependent EIF2AK3 activation compromises ursolic acid-induced apoptosis through upregulation of MCL1 in MCF-7 human breast cancer cells. *Autophagy.* 2013;9(2):196–207. <https://doi.org/10.4161/auto.22805>.
 30. Yan W, Ma X, Zhao X, Zhang S. Baicalein induces apoptosis and autophagy of breast cancer cells via inhibiting PI3K/AKT pathway in vivo and vitro. *Drug Des Devel Ther.* 2018;12:3961–72. <https://doi.org/10.2147/DDDT.S181939>.
 31. Newton K, Manning G. Necroptosis and inflammation. *Annu Rev Biochem.* 2016;85(1):743–63. <https://doi.org/10.1146/annurev-biochem-060815-014830>.

Publisher's Note

Springer Nature remains neutral with regard to jurisdictional claims in published maps and institutional affiliations.

Ready to submit your research? Choose BMC and benefit from:

- fast, convenient online submission
- thorough peer review by experienced researchers in your field
- rapid publication on acceptance
- support for research data, including large and complex data types
- gold Open Access which fosters wider collaboration and increased citations
- maximum visibility for your research: over 100M website views per year

At BMC, research is always in progress.

Learn more biomedcentral.com/submissions

